2013-08-02

Proteasome inhibition and ROS generation by 4-nerolidylcatechol induces melanoma cell death

PIGMENT CELL & MELANOMA RESEARCH, MALDEN, v. 25, n. 3, pp. 354-369, MAY, 2012
http://www.producao.usp.br/handle/BDPI/36330

The official journal of
INTERNATIONAL FEDERATION OF PIGMENT CELL SOCIETIES · SOCIETY FOR MELANOMA RESEARCH
PIGMENT CELL & MELANOMA Research

Proteasome inhibition and ROS generation by 4-nerolidylcatechol induces melanoma cell death

Carla A. Brohem, Renato R. Massaro, Manoela Tiago,Camila E. Marinho, Miriam G. Jasiulionis, Rebeca L. de Almeida, Diogo P. Rivelli, Renata C. Albuquerque, Tiago F. de Oliveira, Ana P. de Melo Loureiro, Sabrina Okada, María S. Soengas, Silvia B. de Moraes Barros and Silvya S. Maria-Engler

DOI: 10.1111/j.1755-148X.2011.00992.x
Volume 25, Issue 3, Pages 354-369

Proteasome inhibition and ROS generation by 4-nerolidylcatechol induces melanoma cell death

Carla A. Brohem[1], Renato R. Massaro[1], Manoela Tiago[1], Camila E. Marinho[1], Miriam G. Jasiulionis[2], Rebeca L. de Almeida[1], Diogo P. Rivelli[1], Renata C. Albuquerque[1], Tiago F. de Oliveira[1], Ana P. de Melo Loureiro[1], Sabrina Okada[1], María S. Soengas[3], Silvia B. de Moraes Barros[1] and Silvya S. Maria-Engler[1]

1 Department of Clinical Chemistry & Toxicology, School of Pharmaceutical Sciences, University of São Paulo, São Paulo, Brazil **2** Pharmacology Department, Federal University of São Paulo, São Paulo, Brazil **3** Centro Nacional de Investigaciones Oncológicas (Spanish National Cancer Research Center) Madrid, Spain

CORRESPONDENCE Silvya S. Maria-Engler, e-mail: silvya@usp.br

KEYWORDS 4-nerolidylcatechol/melanoma/apoptosis/Noxa/proteasomal inhibitor/artificial skin

PUBLICATION DATA Received 5 May 2011, revised and accepted for publication 17 February 2012, published online 28 February 2012

doi: 10.1111/j.1755-148X.2012.00992.x

Summary

Induction of apoptotic cell death in response to chemotherapy and other external stimuli has proved extremely difficult in melanoma, leading to tumor progression, metastasis formation and resistance to therapy. A promising approach for cancer chemotherapy is the inhibition of proteasomal activity, as the half-life of the majority of cellular proteins is under proteasomal control and inhibitors have been shown to induce cell death programs in a wide variety of tumor cell types. 4-Nerolidylcatechol (4-NC) is a potent antioxidant whose cytotoxic potential has already been demonstrated in melanoma tumor cell lines. Furthermore, 4-NC was able to induce the accumulation of ubiquitinated proteins, including classic targets of this process such as Mcl-1. As shown for other proteasomal inhibitors in melanoma, the cytotoxic action of 4-NC is time-dependent upon the pro-apoptotic protein Noxa, which is able to bind and neutralize Mcl-1. We demonstrate the role of 4-NC as a potent inducer of ROS and p53. The use of an artificial skin model containing melanoma also provided evidence that 4-NC prevented melanoma proliferation in a 3D model that more closely resembles normal human skin.

Introduction

Melanoma is the most aggressive skin cancer with the highest mortality. The main risk factor for its development is UV exposure, although individuals with a family history of melanoma have a 30- to 70-fold higher risk of developing the disease (Greinert, 2009; Ibrahim and Haluska, 2009). Metastatic malignant melanoma is largely refractory to chemotherapy and radiotherapy, and has a poor prognosis. The survival rate is of 6 months to 5 yr in <5% of cases. Therefore, efforts to generate new therapeutic strategies are essential (Gray-Schopfer et al., 2007; Hersey and Zhang, 2001; Miller et al., 2009; Paraiso et al., 2010; Soengas and Lowe, 2003; Sorolla et al., 2008).

Although new melanoma treatments such as the B-raf inhibitor (PLX 4032) and the anti-CTLA4 antibody

Significance

4-Nerolidylcatechol (4-NC) is known to induce G1 cell cycle arrest, decrease the activity of MMPs and induce apoptotic cell death. In this study we demonstrate the mechanism of action of this compound starting with the formation and accumulation of ROS, leading to DNA damage, induction of p53, an increase in Noxa that is able to bind and neutralize Mcl-1 followed by poteasomal inhibition, culminating in caspase-dependent apoptosis. Our data now suggest that the 4-NC compound can potentially be used as a chemotherapeutic agent in the treatment of human melanoma.

(IPILIMUMAB) have been associated with a clinical benefit (Flaherty et al., 2010; Hodi et al., 2010), acquired and intrinsic resistance remains a major limiting factor for long-term disease management (Smalley and Sondak, 2010). Current research efforts are focused upon the development of combination therapy strategies and the identification of new classes of therapeutic agents. Another new therapeutic approach for cancer chemotherapy includes pharmacologic inhibitors which, for example, block the ubiquitin-proteasome system and inhibit the autophagy process (Fernández et al., 2006; Jesenberger and Jentsch, 2002; Roberti et al., 2011; Tormo et al., 2009).

In the past decade, pharmacologic inhibitors of the ubiquitin-proteasome pathway have been tested as antitumoral therapeutic agents by inducing cell death both in vitro and in vivo. The inhibition of proteasome activity is expected to be a new strategy for cancer chemotherapy because of its ability to overcome chemoresistant pathways as well as to potentiate the activity of other cancer therapeutics.

The ubiquitin proteasome system (UPS) is responsible for the degradation of the majority of regulatory proteins in eukaryotic cells (Crusio et al., 2010; Nikiforov et al., 2007; Sorolla et al., 2008). Interestingly, many pro-oncogenic factors, e.g. transcriptional factors such as nuclear factor $\kappa\beta$ (NF-$\kappa\beta$), as well as both pro- and anti-apoptotic factors, are also controlled by the proteasome (Crusio et al., 2010; Fernández et al., 2006; Jesenberger and Jentsch, 2002).

4-Nerolidylcatechol (4-NC), a compound initially extracted from the plant *Pothomorphe umbellata* L. Miq (PU), was first described as a potent in vitro antioxidant (Barros et al., 1996). This compound showed high antioxidant activity when compared with α-tocopherol, reported to be one of the most active antioxidants, interfering with one or more steps of the process of propagation of lipid peroxidation (Barros et al., 1996; Desmarchelier et al., 2000). It was demonstrated that the PU compound 4-NC and its antioxidant activity play a significant role in the prevention of damage caused by oxidative stress in skin, suggesting its application in cosmetic formulations (Ropke et al., 2002). In 2002, Ropke and co-workers demonstrated the high percutaneous absorption of 4-NC in a gel formulation (0.1% 4-NC), leading to high levels of the compound in skin. Matrix metalloproteinases (MMPs) 2 and 9 were also inhibited in the presence of 4-NC in a skin photoaging model in mice (Ropke et al., 2006).

We have previously demonstrated the cytotoxic activity of 4-NC in melanoma cell lines. The compound induced G1 cell cycle arrest, decreased MMP activity and induced cell death by apoptosis (Brohem et al., 2009) in melanoma lines in vitro.

In the present work we evaluated the growth inhibitory effects of 4-NC and its ability to induce cell death in a broad panel of cell lines derived from metastatic melanoma, and uncovered a new role of 4-NC as a proteasomal inhibitor. 4-NC induced the accumulation of ubiquitinated proteins, including classic targets of this process such as Mcl-1. As shown for other proteasomal inhibitors in melanoma, the cytotoxic action of 4-NC depended on the pro-apoptotic protein Noxa, which is able to bind and neutralize Mcl-1. We also demonstrate the dual role of 4-NC as a potent ROS inducer. The mechanism of action of this compound, which transpassed the chemoresistance of melanoma cell lines in vitro, is described here in a three-dimensional model of artificial skin.

Results

4-NC cytotoxicity

We have previously reported the cytotoxic activity of 4-NC (structure shown in Figure 1A) in three human metastatic melanoma cell lines and the resistance of normal human fibroblasts to this compound (Brohem et al., 2009).We now demonstrate that this cytotoxic activity extends to a greater number of metastatic melanoma cell lines, irrespective of mutations in p53, BRAF and NRas (Figure 1B), but, interestingly, not for a large panel of human dermal fibroblasts (Supporting Information Figure S1).

Production of reactive oxygen species (ROS) and induction of DNA alterations

Because of the high antioxidant potential attributed to 4-NC (Barros et al., 1996) and the fact that antioxidants also behave as pro-oxidants under certain conditions, we began the mechanistic study of the action of this compound by examining the production of reactive oxygen species (ROS). We measured the activity of two enzymes involved in the cell antioxidant system, catalase and superoxide dismutase (SOD), which are responsible for the maintenance of low levels of ROS and cell homeostasis. As seen in Figure 2A, 4-NC inhibited the action of catalase in both fibroblasts and in melanomas. However, we observed that 4-NC tended to increase the SOD activity only in fibroblasts and not in melanoma cell lines.

Figure 2B demonstrates that the production of the radical superoxide anion ($O_2^{\cdot-}$) by cells is increased in a 4-NC concentration-dependent manner (20, 30, 40, 50 and 100 μM), but each melanoma cell line responds differently. In other words, the pro-oxidant response of the compound depends on the concentration of compound added. Knowing that this compound could induce ROS in melanoma cells, we questioned whether the ROS resulting from 4-NC treatment could induce DNA lesions. To investigate this, we used 8-oxo-7,8-dihydro-2′-deoxyguanosine (8-oxodGuo) as a marker of DNA oxidative damage and phosphorylated histone 2A (γH2AX) as a marker of global DNA damage. The global DNA methylation was verified by quantitation of 5-methyl-2′-

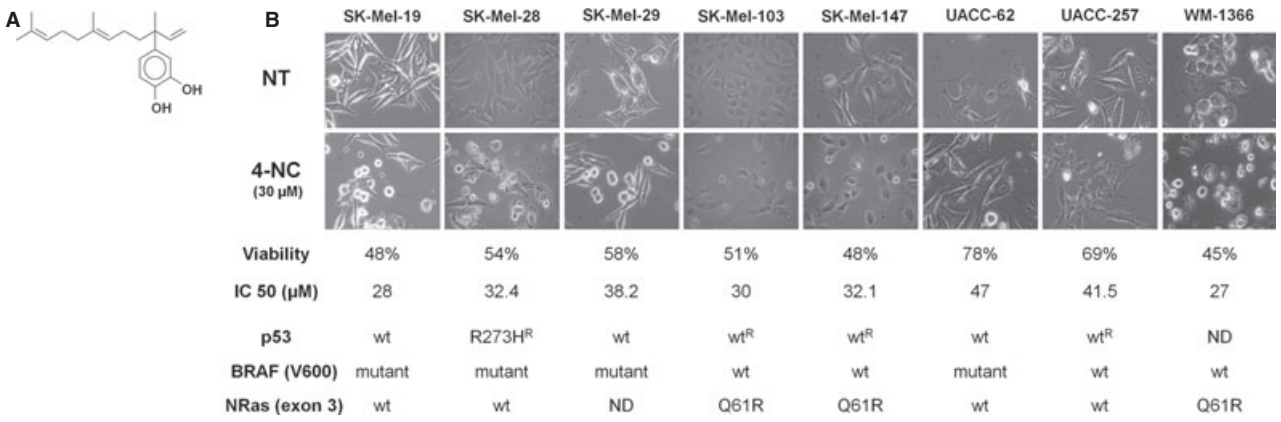

Figure 1. 4-NC-induced cytotoxicity. (A) Structure of 4-nerolidylcathecol (4-NC). (B) 4-NC cytotoxicity in a panel of human metastatic melanoma cell lines at 24 h: SK-Mel-19, SK-Mel-28, SK-Mel-29, SK-Mel-103, SK-Mel-147, UACC-62, UACC-257 and WM-1366. Note that 4-NC shows some cytotoxicity in all cell lines, regardless of mutational status of p53, BRAF(V600) and NRas (exon 3). NT, non-treated. Magnification 40×.

deoxycytidine (5-methyl-dCyd). As shown in Figure 2D, 4-NC induced an increase of 8-oxodGuo and 5-methyl-dCyd levels in SK-Mel-103, in a dose-dependent manner. DNA global damage was also investigated using γH2AX (gamma-H2AX), which can be rapidly phosphorylated due to a DNA double-strand break (Celeste et al., 2003). As seen in Figure 2E, the results of flow cytometry assay show that 30 μM of 4-NC treatment was able to increase the levels of γH2AX.

Reactive oxygen species production was also evaluated via flow cytometric measurement of dichlorofluorescein diacetate (DCFH-DA), a well known compound that quantifies hydrogen peroxide (H_2O_2) produced intracellularly. This probe also indicated a pro-oxidant profile following 4-NC treatment, with increases in ROS production for all cell lines analyzed (Figure 3). ROS production was only detected after 12 h of treatment in normal fibroblasts, but as early as 2 h after treatment in melanoma SK-Mel-28, and production was maintained until 12 h (at 30 μM 4-NC). ROS quantification with the probe DCFH-DA indicated a difference in profile among the cell lines tested. Cell lines SK-Mel-103 and SK-Mel-147 showed dramatic ROS peaks at 2 h after treatment, following both 10 and 30 μM 4-NC treatment, with ROS decreasing after this period (Figure 3).

We used a potent antioxidant compound polyhydroxilic di-sodium 4,5-dihydroxybenzene 1,3-disulfonate (Tiron), which is known to sequester ROS, in order to determine whether 4-NC-induced ROS was responsible for cell death in melanoma cell lines. As shown in the rightpanel in Figure 3, production of H_2O_2 induced by 4-NC was greatly reduced in the presence of Tiron. Addition of Tiron and 4-NC to melanoma cells and normal fibroblasts almost completely abrogated cell death. Thus, we found that the production of ROS induced by 4-NC is essential for its mechanism of action, and that the presence of Tiron prevented 4-NC-induced cell death by approximately 45% in the cell lines studied (left panel, Figure 3). Results regarding Tiron cytotoxic effects are shown in Supporting Information Figure S2.

Evaluation of protein modulation involved in apoptotic cell death

We evaluated the effect of 4-NC on p53 protein (Figure 4) because of the relationship of the nuclear phosphoprotein p53 with oxidative stress and its key role in maintaining genome integrity via DNA repair or removal of damaged cells through apoptosis. 4-NC caused an increase in p53 protein levels in melanoma cell lines SK-Mel-103 and SK-Mel-147, which maintain wild-type p53. As expected, p53 levels in the cell line SK-Mel-28 (mutant p53) were not altered. Furthermore, human fibroblasts, which are much less sensitive to 4-NC treatment, demonstrated almost no increase in p53 under these conditions (see graphic quantification in Figure 4).

Key regulators of the intrinsic apoptotic pathway were also analyzed, including the anti-apoptotic Bcl-2 family members, in the absence or presence of 4-NC. As can be seen in Figure 5A, 4-NC does not appear to regulate Bcl-2 and Bcl-xL protein levels in melanoma cell lines. Conversely, levels of the anti-apoptotic Mcl-1 family member were increased. Furthermore, 4-NC was able to further modulate pro-apoptotic proteins of the Bcl-2 family, inducing the cleavage of Bax and Bid as well as the upregulation of Noxa (Figure 5B).

Interestingly, this increase in both the anti-apoptotic Mcl-1 (Figure 5A) and pro-apoptotic Noxa (Figure 5B) reflected a pattern very similar to that exhibited by melanoma cells following treatment with bortezomib, a known proteasome inhibitor. Using bortezomib as a control, we discovered that not only were levels of Noxa and Mcl-1 increased following treatment with 4-NC, but there was also an accumulation of ubiquitinylated pro-

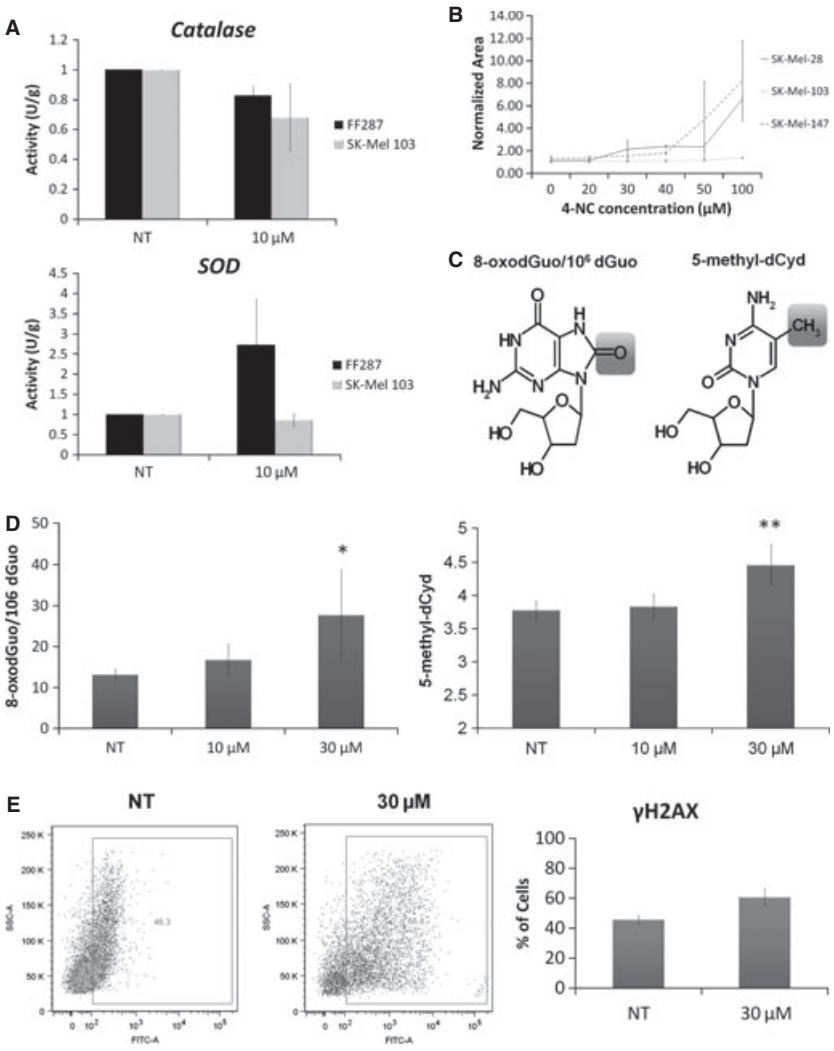

Figure 2. 4-NC modulates antioxidant enzymes, inducing ROS and DNA damage. (A) Measurement of enzyme activity for catalase and SOD in fibroblasts (FF287) and metastatic melanoma cell line SK-Mel-103 in the presence (10 μM) or absence (NT) of 4-NC. (B) Lucigenin detection of superoxide radical ($O_2^{\cdot-}$) after the addition of 4-NC (20, 30, 40, 50 and 100 μM) in human melanoma cell lines: SK-Mel-28, SK-Mel-103 and SK-Mel-147. The analysis was performed following exposure to 4-NC for 30 min. (C) Molecular structure of 8-oxodGuo/106 dGuo and 5-methyl-dCyd. (D) DNA lesions induced by 4-NC in SK-Mel-103 measured by %8-oxodGuo/106 dGuo and %5-methyl-dCyd after the addition of 4-NC (10 and 30 μM). (E) DotPlot and histogram of γH2AX phosphorylation in SK-Mel-103 NT and in the presence of 4-NC (30 μM). NT, non-treated. 10 = treated with 10 μM of 4-NC. 30 = treated with 30 μM of 4-NC. *P < 0.05; ***P < 0.001.

teins in the cell extracts, possibly suggesting that 4-NC acts at the proteasomal level. We extended our analysis of Bcl-xL, Mcl-1 and Noxa levels to include melanocytes, keratinocytes and the p53 mutant melanoma cell line SK-Mel-28. Comparing these lines with SK-Mel-147, although 4-NC induced Mcl-1 and Noxa levels to some degree in all cell lines studied, there was a more dramatic induction of Noxa in the sensitive melanoma line SK-Mel-147 (Supporting Information Figure S3). The same was shown in the sensitive cell line SK-Mel-103 (Figure 5B).

As the cleavage of Bid and Bax and the increase in pro-apoptotic Noxa contributed to the alteration of mitochondrial membrane potential, we utilized a 3,3′-dihexyloxacarbocyanine iodide ($DiOC_6$) probe for measurement of mitochondrial membrane potential by flow cytometry (Figure 5C). 4-NC induced a change in membrane potential in a dose-dependent manner, showing a release of mitochondrial cytochrome *c* and an activation of the intrinsic apoptotic pathway. This change was more pronounced in melanoma cell line SK-Mel-103, which we have shown is more sensitive to 4-NC treatment (see photos and cell viability in Figure 3).

Immunoblotting demonstrated the cleaved protein product (35 kDa) of caspase-3, as well as those of caspase-9 (37, 35 and 17 kDa) in melanoma cell lines following 24 h treatment with 30 μM 4-NC (Figure 6A). Because fibroblasts are more resistant to the action of 4-NC, this cleavage was not observed following treatment with the compound. The drug doxorubicin was used as a positive control, as it has been widely described in the literature to induce caspase-dependent apoptosis.

To verify that the apoptosis induced by 4-NC was really dependent on caspases, we used the pan caspase inhibitor zVAD-fmk (carbobenzoxy-valyl-alanyl-aspartyl-[O-methyl]-fluoromethylketone). In the presence of zVAD, there is an increase in cell viability even when cells are treated with 30 μM of 4-NC (Figure 6B). We also verified the inhibition of caspase cleavage by immunoblotting in the presence of zVAD and 4-NC (Figure 6B).

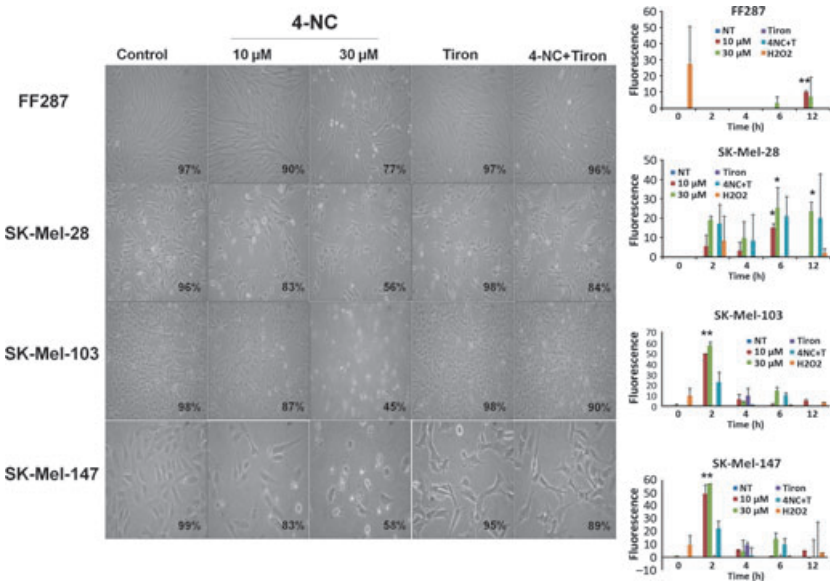

Figure 3. 4-NC induces ROS production in melanoma cells. Right: Detection of 4-NC-induced hydrogen peroxide production with the probe DCFH-DA by flow cytometry. Shown is the ROS-dependent increase in fluorescence (arbitrary units) versus time for the cell lines FF287, SK-Mel-28, SK-Mel-103 and SK-Mel-147 after the addition of 4-NC (10 and 30 μM), Tiron (1 mM) and mixed (30 μM 4-NC and 1 mM Tiron). We used H_2O_2 as a control for the reaction. *P < 0.05 and **P < 0.001. Left: Optical micrographs of the cell lines according to the conditions described above. Control = untreated. Cell viability in the presence or absence of each treatment is indicated.

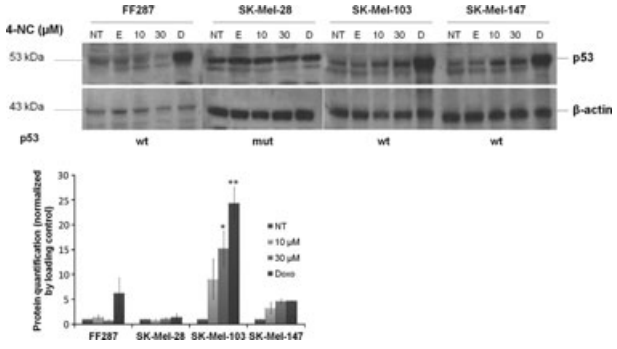

Figure 4. 4-NC-induced p53 stabilization. Evaluation of p53 protein expression in normal cells: FF287 (fibroblasts); and metastatic melanomas: SK-Mel-28, SK-Mel-103 and SK-Mel-147, following 4-NC (10 or 30 μM) treatment as compared with non-treated (NT). The chemotherapeutic agent doxorubicin (0.8 mg/ml) was used as control. wt, wild-type; mut, mutated *p53* gene. The protein actin was used as a protein quantification control. Quantification of p53 induction by doxorubicin or 4-NC is shown on the right. *P < 0.05; **P < 0.01.

Figure 6C demonstrates that the caspase-dependent apoptosis by 4-NC and Noxa upregulation are related to ROS production. The joint treatment of Tiron and 4-NC in SK-Mel-103 does not induce caspase cleavage or Noxa accumulation. Our results indicate that treatment with 4-NC induces caspase-dependent apoptosis in the melanoma cell lines studied and also that the production of ROS induced by 4-NC is essential for its mechanism of action. In addition, a proteasome inhibitor, MG132, was used as control (cytotoxic results shown in Supporting Information Figure S4), whose activity is not influenced by the presence of Tiron; this led us to perform experiments concerning proteasomal inhibition.

Identifying 4-NC as a proteasome inhibitor

Interestingly, upon analyzing the key apoptotic regulators by immunoblotting, we discovered that treatment with 4-NC led to a dramatic increase in the protein levels of Noxa and Mcl-1. This pattern is a similar to that previously seen in melanoma after bortezomib-induced cell death (Fernández et al., 2005, 2006; Nikiforov et al., 2007). As bortezomib is a proteasome inhibitor, we decided to investigate the proteasomal activity in the melanoma cells treated with the 4-NC compound. We observed a dramatic increase in ubiquitinylated proteins at both 10 and 30 μM concentrations of 4-NC (Figure 7A). This is an indication of proteasomal inhibition and we used bortezomib treatment as a positive control (shown in far right lane). It is noteworthy that the accumulation of ubiquitinylated proteins in normal fibroblasts, which are more resistant to 4-NC killing, was much less dramatic than in melanoma lines.

As shown in Figure 7B, 4-NC was able to inhibit proteasomal activity in an extremely significant manner. Measurement of the proteasomal activity via detection of the fluorophore 7-amino-4-methylcoumarin (AMC) indicated that SK-Mel-103 and SK-Mel-147 cell lines have higher levels of proteasome activity as compared with fibroblasts and SK-Mel-28. Although there were differences in proteasomal activity among the cell lines, 4-NC inhibited the proteasomal activity at 10 and 30 μM in all cell lines. At the higher concentrations, 4-NC inhibited the proteasome activity of all cell lines analyzed in a manner very similar to that of the proteasome inhibitor bortezomib.

To determine whether 4-NC-induced cell death was dependent on upregulation of Noxa, which in turn could neutralize high Mcl-1 levels, we used lentiviral vectors containing shRNAs directed against Noxa to assess the role of NOXA protein in cell death. As shown in Figure 7B, 4-NC-induced cell death was almost com-

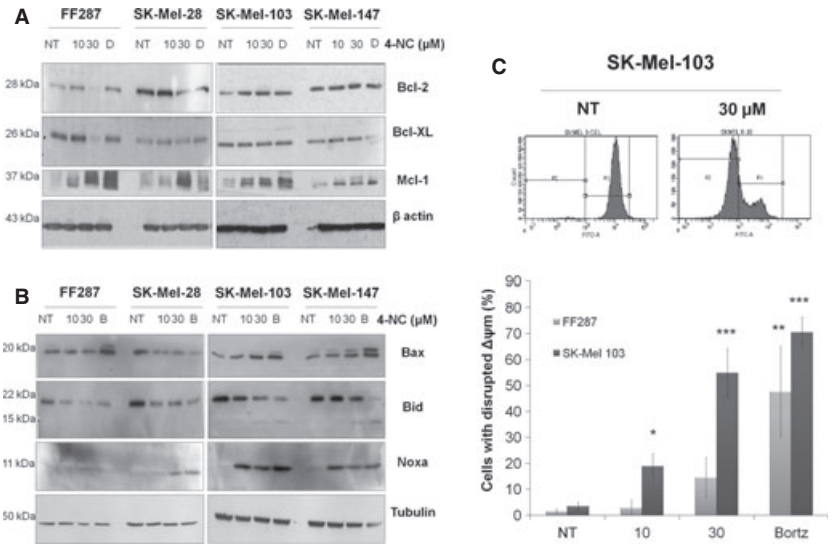

Figure 5. 4-NC induces apoptosis and modulates pro- and anti-apoptotic proteins. Evaluation of protein expression of (A) anti-apotic proteins: Bcl-2, Bcl-xL and Mcl-1, and expression/cleavage patterns of (B) pro-apoptotic proteins Bid, Bax and Noxa, in normal cells: FF287 (fibroblasts) and metastatic melanoma: SK-Mel-28, SK-Mel-103 and SK-Mel-147, untreated (NT) or treated with 4-NC (10 and 30 μM) for 24 h. D, doxorubicin; B, bortezomib, drugs used as control. β-actin or tubulin proteins were used as protein quantification controls. (C) Change of mitochondrial membrane potential ($\Delta\psi$m) treatment with 4-NC (10 and 30 μM), verification by the probe DiCO6 (3) by flow cytometry (FITC-reading). Note the greatest peak change in the melanoma cell line SK-Mel-103. *P < 0.05; **P < 0.01;***P < 0.001.

pletely abrogated following downregulation of Noxa by shRNA in melanoma line SK-Mel-103. In the absence of Noxa, 4-NC was unable to induce cell death by apoptosis. Cell viability in SK-Mel-103 increased from 51% in the presence of 30 μM 4-NC to 78% (shNoxa1) and 94% (shNoxa2) upon Noxa inhibition. This demonstrates the importance of the Noxa gene in the mechanism of action of 4-NC. We performed Western blotting assays to detect Noxa protein half-life after 4-NC treatment. 4-NC induced Noxa accumulation at all time points studied: 3, 6, 12, 24 and 48 h after treatment. In the presence of Tiron as well, 4-NC was not able to induce Noxa production, showing the relation of Noxa accumulation and ROS (data not shown).

Action of 4-NC in an artificial skin model containing melanoma

To evaluate the action of 4-NC in a 3D model more closely reproducing normal skin than in vitro monolayer cell cultures, we cultivated the metastatic melanoma cell line (SK-Mel-103) in a model of reconstructed artificial skin. As shown in Figure 8A, when metastatic melanoma is included in the reconstructed artificial skin and grown with other components of the epidermis (melanocytes and keratinocytes), there is a marked epidermal hyperplasia due to proliferating melanoma cells. In the presence of melanoma, the top differentiated epidermal layers did not appear after 15 days of culture and numerous melanoma foci grew vertically into the underlying dermal layer. (Figure 8, control without melanoma and NT). When the skin containing melanoma (Figure 8) was treated with 10 μM of 4-NC for 72 h, the melanoma proliferation appeared reduced as compared with the control, resulting in a thinner epidermal layer with fewer melanoma foci growing vertically into the dermal layer (Figure 8, middle panels). Upon treatment with 30 μM of 4-NC, these effects became much more prevalent. There was a reduced presence of melanoma proliferation in the epidermis with no vertical growth observed into the underlying dermal layer (Figure 8, right panels). The epithelium differentiation markers keratin 14 (Figure 8B) and involucrin (Figure 8C) were used to identify the basal and upper layers of the skin, respectively. These markers were used to observe undifferentiated epithelia, as well as areas of melanoma growth (arrows) and regression with 4-NC treatment. Note that in this 3D model, 4-NC was not toxic for normal keratinocyte cells, once the epidermis was able to proliferate in the presence of 30 μM of 4-NC.

Discussion

In 1926, the first edition of the Brazilian Pharmacopeia (Silva, 1926) registered the roots of *Pothomorphe umbellata* L. Miq as a drug that had been used for a long time in traditional Brazilian medicine. The use of *P. umbellata* in traditional medicine includes the treatment of several diseases and the pharmacological proprieties of this plant were attributed to its main compound, 4-neroldylcatechol. The plant extract containing 4-NC has been long employed, including in the treatment of skin-related injuries, and the non-toxic effects on normal skin cells have been noted and described.

4-NC was initially described as a potent antioxidant (Barros et al., 1996). However, it has more recently been shown to have cytotoxic potential against human metastatic melanoma cells (Brohem et al., 2009). The development and progression of melanoma can also be the result of oxidative stress in skin melanocytes (Meyskens et al., 2001; Nihal et al., 2005), and under certain conditions antioxidants can act as pro-oxidants (Chandan, 2002; Dong et al., 2007; Nakazato et al., 2005). Therefore we hypothesized that 4-NC properties potentially could be useful for controlling melanoma tumor progression.

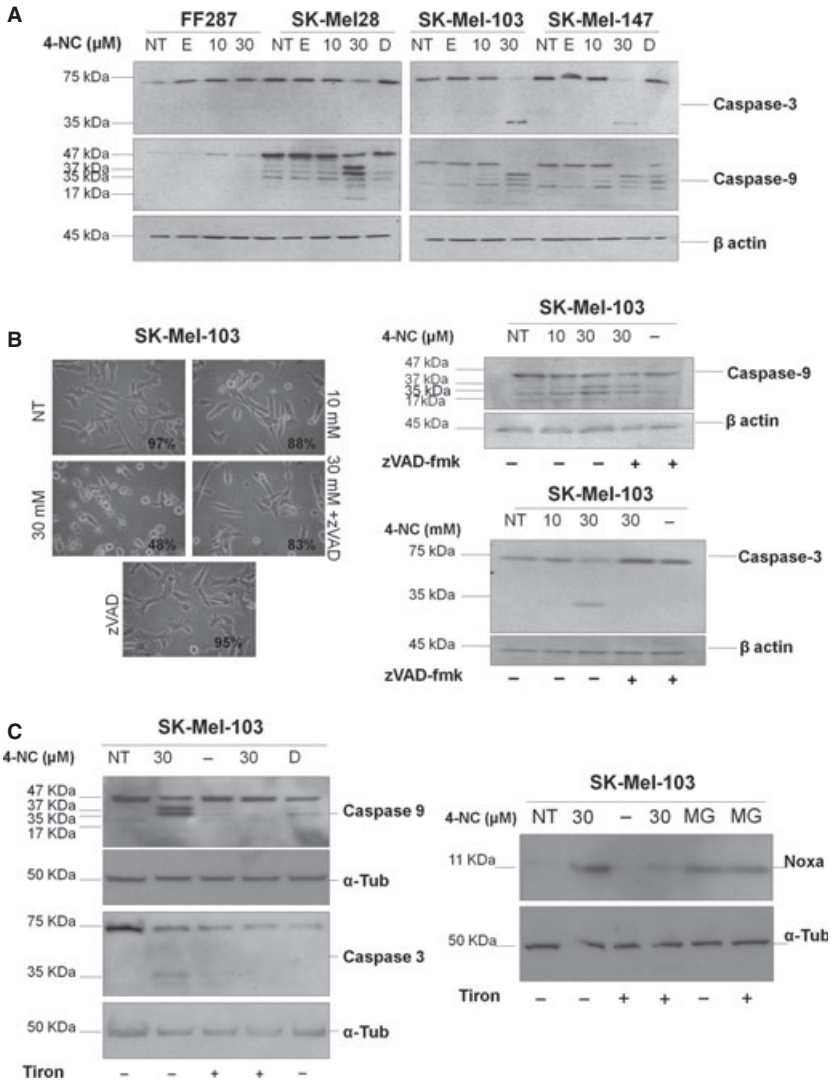

Figure 6. Caspase-dependent cell death. (A) Evaluation of caspase-3 and caspase-9 cleavage in normal cells [FF287 (fibroblasts] and metastatic melanomas (SK-Mel-28, SK-Mel-103 and SK-Mel-147) following 4-NC (10 or 30 μM) treatment as compared with non-treated (NT) for 24 h. E = 1% ethanol control, D = doxorubicin 0.5 mg/ml for 24 h. The protein β-actin was used as a loading control. (B) Effects of caspase inhibition as shown by light microscopy (left panel) on the melanoma line SK-Mel-103 treated with 4-NC (10 and 30 μM) in the presence and absence of the pan-caspase inhibitor zVAD-fmk at 24 h. Cell viability as determined by Trypan Blue exclusion assay is indicated. Effects on caspase-9 and caspase-3 cleavage patterns are shown by immunoblotting (right panel) for SK-Mel-103, in the absence (–) or presence (+) of zVAD. β-actin was used as a loading control. (C) Evaluation of caspase-3 and caspase-9 cleavage in SK-Mel-103, in the presence (+) or absence (–) of Tiron when not treated (NT) or treated with 4-NC 30 μM (right panel); and also Noxa expression levels (left panel) in the same conditions; the proteasome inhibitor MG132 (MG) was used as control. α-Tubulin was used as a loading control.

We initially treated a panel of melanoma cell lines as well as normal cells with 4-NC to determine the effects of 4-NC on cell viability. 4-NC induced cell death in all melanoma cell lines that contained different point mutations in genes such as p53, BRAF and NRas, showing an important feature of this compound. The treatment lasted 24 h in these studies, confirming the results of Brohem et al. (2009), which showed the efficacy of 4-NC.

To determine whether 4-NC played any role in ROS regulation in the melanoma cell lines studied, we assessed the activity of two enzymes involved in the REDOX cell system, specifically catalase and superoxide dismutase (SOD). 4-NC was able to inhibit the enzyme catalase in fibroblasts and human melanomas. Catalase is a well conserved enzyme among organisms which detoxifies hydrogen peroxide into water and oxygen (Nishikawa et al., 2005). Mechanistic studies of compounds that induce apoptotic cell death via ROS have demonstrated the importance of inhibition of this enzyme in the accumulation of ROS and, consequently, cell death by apoptosis. A study published by Averill-Bates et al. (2008) showed that polyamine cytotoxicity in murine melanoma B16-F10 occurs only upon concurrent catalase inhibition, demonstrating the importance of ROS accumulation in melanoma cell death (Averill-Bates et al., 2008).

The superoxide anion ($O_2^{\cdot-}$) can result from mitochondrial respiratory chain activity, and mitochondria contain active superoxide dismutase (SOD) (Koch et al., 2004) to protect mitochondria from damage by free radicals (Pani et al., 2009a). Therefore, we also analyzed this enzyme of the antioxidant system. We found that 4-NC was able to induce an increase of SOD activity in fibroblasts but not in melanomas. An increase of antioxidant enzymes can be associated with suppression of tumorigenicity and metastatic ability in some tumors (Rieber and Rieber, 1999). Therefore, the increased SOD activity in fibroblasts upon 4-NC treatment might explain the resistance of these cells to 4-NC, i.e. not allowing the accumulation of superoxide anion radical, and therefore not causing mitochondrial damage leading to apoptosis.

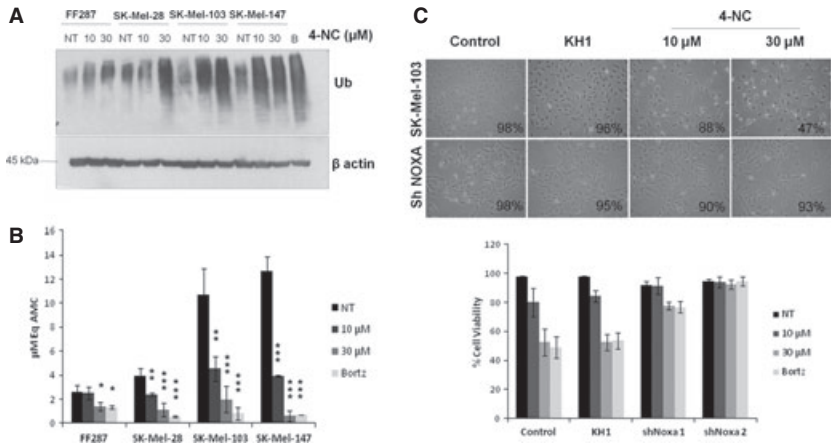

Figure 7. 4-NC cytotoxicity is dependent on proteasomal activity and Noxa. (A) Protein ubiquitinylation after 24 h of 4-NC treatment (10 or 30 μM). (B) Inhibition of proteasomal activity by treatment with 4-NC. Proteasomal activity is measured by detection of the fluorophore 7-amino-4-methylcoumarin (AMC). 4-NC was able to inhibit proteasomal activity in all cell lines after 24 h treatment (10 or 30 μM). (C) Optical microscopy of melanoma SK-Mel-103 following shRNA downregulation of Noxa in the presence or absence of 4-NC treatment (10 or 30 μM) as compared with non-treated (NT) or bortezomib (Bortz) control. Cell viability as determined by Trypan Blue exclusion assay is indicated at 24 h. Bottom panel indicates quantification of % cell viability for control, *uninfected cells*; KH1, *lentiviral control infected cells*; shNoxa 1 and 2, *two separate shRNA constructs designed to recognize nucleotides of the Noxa gene*, following 4-NC treatment (10 or 30 μM) as compared to non-treated (NT), or bortezomib (Bortz)-treated. *P < 0.05; ** P < 0.01; ***P < 0.001.

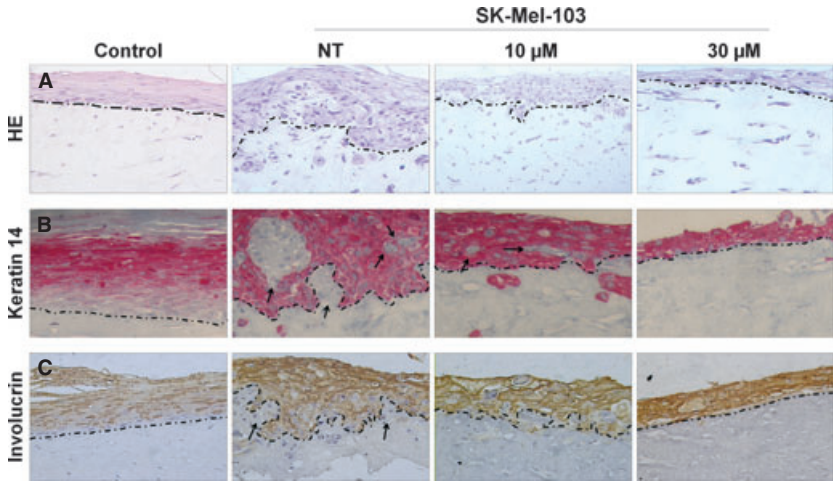

Figure 8. 4-NC inhibits metastatic melanoma invasion in an artificial skin model. (A) H&E staining. (B) Immunostaining for keratin 14 and (C) involucrin following 4-NC treatment for 72 h. Control – artificial skin without addition of melanoma. NT – artificial skin in the presence of melanoma cell line SK-Mel-103 with no 4-NC treatment, or treated at concentrations of 10 or 30 μM. Arrows indicate regions of melanoma proliferation. (A) 20×, (B) 40× magnification.

Increased ROS generation can lead to biomolecular damage, which may contribute to cell death. A useful marker of cell oxidative damage is the lesion 8-oxodGuo, generated by guanine one-electron oxidation and through ·OH radical or singlet oxygen ($^1O_2$) attack to the guanine moiety in DNA (Cadet et al., 2008). The lesion 8-oxodGuo has been widely used as a marker of oxidative stress in epidemiologic and mechanistic studies (Bianchini et al., 2001; Cadet et al., 2008; Chuang et al., 2010; Li et al., 2010; Yoshino et al., 2002) and lately there have been efforts to minimize its artifactual generation during DNA preparation for analysis (Chao et al., 2008; ESCODD, 2002; ESCODD et al., 2004; Mangal et al., 2009; Ravanat et al., 2002). 4-NC (30 μM) increased by about twofold the levels of 8-oxodGuo in SK-Mel-103 cells, as measured by HPLC-ESI-MS/MS (Figure 2D), indicating that ROS production affects cell DNA, leading to lesions that may trigger apoptosis (Chuang et al., 2010; Li et al., 2010).

This compound caused global DNA damage, increasing the phosphorylation of gamma-H2AX (γH2AX)-positive cells (Figure 2E). The genotoxic effect of several substances can be detected by analysis of γH2AX expression, as is evidenced by the checkpoint response to DNA double-strand breaks (Gaddameedhi and Sancar, 2011). Clinical samples from cancer patients were evaluated for γH2AX levels, showing that these can be used as markers for treatment efficiency and prediction of tumor cell sensitivity to DNA damage of new drugs (Podhorecka et al., 2010).

Besides genotoxicity, 4-NC (30 μM) altered the global DNA methylation pattern of SK-Mel-103 cells, inducing DNA global hypermethylation. DNA methylation occurs in the C-5 position of cytosine and is a stable epigenetic event crucial for normal proliferation and maintenance of genomic stability. It is suggested that the DNA methylation pattern can be changed by exposure to genotoxic agents, with transmission of the new pattern to the subsequent cell generations (Yauk et al., 2008). DNA methyl-transferases (DNMTs) are the enzymes that accomplish the C-5 cytosine methylation in DNA. These enzymes are upregulated when DNA is damaged and their DNA binding affinity is better when DNA lesions are present (James et al., 2003). It is hypothesized that DNMT1 is an ancient DNA repair enzyme conserved throughout the evolution and its upregulation when DNA is damaged leads to DNA hypermethylation (Roberts, 1995; Yauk et al., 2008). DNA hypermethylation may alter chromatin structure and decrease gene expression, among other effects (Yauk et al., 2008), which may change the rates of cell replication and survival.

An increase in the total amount of ROS was observed following the treatment with 4-NC in melanoma cell lines with both detection probes. As a control, the potent antioxidant Tiron was used in combination with 4-NC. This antioxidant was used because there are studies that indicate that Tiron can inhibit apoptosis in melanoma when the melanoma is caused by ROS induced by cytotoxic compounds, such as bortezomib (Fernández et al., 2006), or combination therapies such as MAPK inhibitor and BH3 mimetics (Verhaegen et al., 2006). The combination of 4-NC and Tiron reduced cell death quite dramatically compared with treatment with 4-NC only. This is an indication that the possible mechanism of action of 4-NC begins with the production of ROS, eventually leading to cell death. The ROS production increment begins after 12 h for fibroblast after treatment, whereas in melanoma it occurs after just 2 h of 4-NC exposure. This may partially explain the resistance of fibroblasts to this compound at the evaluated time points, suggesting a possible therapeutic window for treatment. Among the melanomas, we also observed profile differences; cell lines SK-Mel-103 and SK-Mel-147 demonstrated the highest ROS peak at 2 h after treatment, with levels dropping soon afterwards. In contrast, there is a constant induction of ROS in cell line SK-Mel-28 throughout the exposure to 4-NC.

An explanation for this difference may stem from the fact that SK-Mel-28 has a point mutation in codon 145 of the p53 gene, causing overexpression of a mutant protein (Girnita et al., 2000; Haapajarvi et al., 1999; Mousavi-Shafaei et al., 2009), which has been shown to positively regulate genes crucial for tumor transformation and maintenance of tumorigenicity in melanoma, such as insulin-like growth factor I receptor (IGF-IR). In cells where p53 remains a wild type, the opposite occurs, i.e. p53 inhibits the transcriptional regulation of this gene (Girnita et al., 2000). It is also known that p53 is able to induce the production and accumulation of ROS by promoting mitochondrial oxidative stress via expression of p66shc protein, generating a mitochondrial hydrogen peroxide (Pani et al., 2009a,b). Thus, the fact that SK-Mel-28 has a gain of function mutation in p53 possibly leads to an increased accumulation of ROS, due to the induction of mitochondrial oxidative stress.

These results indicated a divergent role for 4-NC, not acting as an antioxidant in this setting, but rather inducing the production of ROS in melanoma cell lines. This may be because some antioxidants assume the characteristics of a pro-oxidant such as vitamin E and ECGC, under certain conditions, such as a strong oxidizing environment where there is lack of support for the regeneration (reduction) of oxidized antioxidants (Chandan, 2002; Dong et al., 2007; Nakazato et al., 2005).

Reactive oxygen species are known to play a role in the regulation of the intrinsic pathway of apoptosis (Li et al., 2002; Pani et al., 2009a; Ribeiro et al., 2005; Sies, 1993). We have previously described the 4-NC induction of cell death by apoptosis in melanoma cell lines (Brohem et al., 2009) and we have furthermore shown that 4-NC induces ROS production (Figure 3) as well as DNA lesions (Figure 2D, E). We then asked whether 4-NC was indeed inducing apoptosis via accumulation of the critical tumor suppressor p53, which is known to have multiple downstream targets that play key roles in cell death. 4-NC treatment did indeed allow accumulation of p53 in the melanoma cell lines SK-Mel-103 and SK-Mel-147, which retain wild-type p53. There is no accumulation of p53 in normal fibroblasts, and they are more resistant than 4-NC-induced cells.

Once activated, p53 can induce the expression of multiple transcriptional downstream targets, including members of pro-apoptotic Bcl-2 family members such as BAX, Puma and Noxa. These factors contribute to changes in mitochondria physiology that favor the release of cytochrome *c* and imminent cell death. 4-NC induced upregulation of the pro-apoptotic protein Noxa, as well as the cleavage of other pro-members including Bax and Bid (Figure 5B), a pattern typically seen upon induction of apoptotic cell death. Opposed to pro-apoptotic protein functions are the anti-apoptotic Bcl-2 family members (e.g. Bcl-2, Bcl-xL, Mcl-1) (Gray-Schopfer et al., 2007; Hersey and Zhang, 2001; Ibrahim and Haluska, 2009; Soengas and Lowe, 2003). 4-NC treatment had no effect on Bcl-2 and Bcl-xL members. However, there was an increase in the anti-apoptotic family member Mcl-1 in all cell lines tested.

Overexpression of Noxa in many types of cancer is associated with its localization to mitochondria, leading to apoptotic cell death. Mcl-1 is an ubiquitin target that is upregulated when the proteasome is inhibited. However, Noxa has the ability to bind specifically to Mcl-1,

hence neutralizing its anti-apoptotic functions and inducing apoptosis (Miller et al., 2009; Nikiforov et al., 2007; Oda et al., 2000; Ploner et al., 2008). Although treatment with 4-NC was able to induce high levels of Mcl-1, the accumulation of Noxa in the sensitive melanoma cell lines studied most likely neutralized this protein, leading to cell death (Figure 5B).

Increases in pro-apoptotic proteins can lead to changes in mitochondrial outer membrane potential (MOMP) with subsequent release of cytochrome *c* and activation of downstream signaling in the intrinsic apoptotic pathway. We observed that 4-NC altered the mitochondrial membrane potential more drastically in melanomas than in normal fibroblasts. This suggests that there is a release of cytochrome *c* from the mitochondria into the cytoplasm, which together with Apaf-1 and caspase-9 leads to the formation of the apoptosome and downstream cell death (Soengas and Lowe, 2003).

The proforms of caspases are inactive and when cleaved in the cytosol, activation occurs, enabling them to cleave/degrade several proteins that are required for cell function. Figure 6A shows cleavage of caspase-3 and caspase-9 in human melanoma lines when treated with 30 μM of 4-NC for 24 h. Because fibroblasts are more resistant to the action of 4-NC, this cleavage was not observed when treated with a concentration of the compound at this time point, indicating a possible therapeutic window for treatment. To ensure that caspase cleavage and activation is required for 4-NC-induced apoptosis, assays with a pan-caspase inhibitor known as Z-VAD-FMK [carbobenzoxy-valyl-alanyl-aspartyl-(O-methyl)-fluoromethylketone] were performed. This compound can permeate cells and bind irreversibly to the catalytic site of caspases, inhibiting the induction of apoptosis. When Z-VAD-FMK was present, the cells were resistant to 4-NC action, cell death was reduced and caspase cleavage was no longer observed (Figure 6B). This proves that 4-NC-induced cell death occurs in a caspase-dependent fashion.

The fact that, in the presence of Tiron, 4-NC was not able to induce caspase cleavage and Noxa overexpression also shows that the ROS production is essential for 4-NC mechanism of action.

Optimal proteasomal function is essential for survival of melanoma cells (Amiri et al., 2004; Chen et al., 2009; Fernández et al., 2006; Wolter et al., 2007), indicating that targeting proteasomal regulation may be a potential therapeutic target. Bortezomib (Velcade®; Janssen, Titusville, NJ, USA), a proteasomal inhibitor, has been widely studied as a possible chemotherapeutic agent in the treatment of melanoma (Fernández et al., 2005, 2006; Lecis et al., 2010; Sorolla et al., 2008; Su et al., 2010; Wolter et al., 2007). Unfortunately, bortezomib was not as effective and was very toxic in clinical trials when used as a single agent (Markovic et al., 2005; Tawbi and Nimmagadda, 2009), which has prompted the study of combination therapy of this agent with other chemodrugs (Seeger et al., 2010; Sorolla et al., 2008; Su et al., 2010). For example, there is an ongoing phase I/II trial of melanoma patients with advanced solid tumors treated with bortezomib and temozolomide (Su et al., 2010).

As 4-NC induces the accumulation of ubiquitinylated proteins, with the accumulation of Noxa and Mcl-1, this led us to test whether 4-NC acts as a proteasome inhibitor in melanoma cell lines. Regarding intracellular proteasomal activity, we have shown that 4-NC does indeed act as a proteasome inhibitor. Melanoma cell lines SK-Mel-103 and SK-Mel-147 have higher levels of proteasome activity when compared with normal fibroblasts. 4-NC was able to inhibit this proteasomal activity even at the lowest concentration (10 μM) in these two cell lines and also in SK-Mel-28. At the higher concentration, 4-NC was able to inhibit the proteasome activity of all cell lines analyzed in a very similar fashion to bortezomib.

Identification of 4-NC as a proteasomal inhibitor may also explain the high levels of ROS, as proteasomal inhibitors can lead to increase in ROS. However, the mechanism responsible for the generation of ROS after inhibition of the proteasome is not known. It has been proposed that the generation of ROS by bortezomib may be due to induction of superoxide and changes in the oxidation-reduction pathway due to interference with mitochondrial electron transport or by endoplasmic reticulum stress due to accumulation of proteins in this organelle (Pérez-Galán et al., 2006).

The pro-apoptotic protein Noxa is the first target induced by the proteasome inhibitor bortezomib in cancer cells (Nikiforov et al., 2007; Wolter et al., 2007). For this reason, we also tested whether Noxa was essential for the apoptosis induced by 4-NC. The cells exhibiting Noxa downregulation were resistant to 4-NC treatment, implicating this protein as an important target of 4-NC in melanoma cell lines. With this data, we can now classify 4-NC as a new proteasome inhibitor triggering apoptosis in various metastatic melanoma cell lines irrespective of background mutations.

An additional point always to consider when studying and designing novel cancer therapy is that cancer is a heterogeneous disease where cell–cell and cell–matrix interactions play an important role in the initiation and progression of tumor development and metastasis. In the past few years, 3D culture models have been incorporated as sophisticated models in the study of tumor biology. The 3D assay is becoming the model of choice because it recreates a species-specific model mimicking the tumor microenvironment (Brohem et al., 2010; Chioni and Grose, 2008). For these reasons, we employed this important model in the study of the effects and mechanism of action of 4-NC in a cell–matrix context. The 4-NC compound was determined to have no cytotoxic effects on the dermal equivalent (Supporting Information Figure S5) but was able dramatically to inhibit melanoma proliferation after 72 h of treatment and allowed normal cells to proliferate in the epithelium (Figure 8).

The data presented show that 4-NC has several capabilities as an anti-tumoral compound and that proteasome inhibition is only one aspect of the complicated pharmacology of this compound. PU has been used in traditional medicine to treat cutaneous injuries, so one future application for 4-NC could be as a topical therapy for patients with cutaneous metastases. As this compound works in NRas melanoma cell lines and cutaneous NRas mutant melanomas tend to arise in older patients (Thomas et al., 2007), who are often not good candidates for surgery or aggressive chemotherapy, 4-NC could be one approach to local disease control.

Local lesion destruction through the induction of apoptosis can also be beneficial, as it can enhance immune recognition of the untreated lesions, the so-called bystander effect (BE). This effect is mediated by cytokines and ROS released from cancer cells (Merle et al., 2008). For instance, in murine experiments, after treatment of primary tumors with chloroethylnitrosourea (CENU), an anticancer agent that acts via DNA damage, secondary tumors that were not treated exhibited growth inhibition and metabolism disorders. In other words, the secondary untreated tumor response was considered the chemotherapy-induced bystander effect (Demidem et al., 2010; Merle et al., 2008).

In conclusion, we have shown that 4-NC, a compound isolated from the Brazilian plant *P. umbellata*, has the ability to transpass the resistance of multiple melanoma cell lines, despite the presence of distinctive mutations in genes conferring resistance to apoptosis. 4-NC induced cytotoxicity in a panel of melanomas via induction of ROS, DNA damage, increased levels of p53 and Noxa, alterations in mitochondrial membrane potential, and ultimately caspase-dependent apoptosis. In addition, we have now uncovered a previously unknown role for 4-NC in proteasomal inhibition. Furthermore, we have shown that 4-NC inhibited melanoma proliferation in a 3D model of artificial skin. Our data explain the mechanism of action of this compound in induction of apoptotic cell death in melanoma and also as a new proteasomal inhibitor which can induce cell death in melanoma.

Methods

4-Nerolidylcatechol isolation

4-NC was isolated from the crude extract of *P. umbellata* as described by Desmarchelier et al. (2000) and Gustafson et al. (1992). The freeze-dried ethanol:water (1:1, v/v) crude extract (10 g) was submitted to a 60 H silica-gel (0.063–0.100 mm) chromatography column (15 mm i.d. × 230 mm) and eluted with $CHCl_2$ (Merck, Darmstadt, Germany) at 23 ml/min in a Buchi flash chromatography liquid system (Switzerland). TLC (thin-layer chromatography) was used to detect the 4-NC, comparing it with the previously isolated 4-NC as a standard and dichloromethane:methanol (91:1 v/v) as the mobile phase. 4-NC (100% purity) was isolated using a Shimadzu SCL 10AVP HPLC system (Kyoto, Japan) equipped with a UV/VIS detector (SPD10A VP–diode array), CLASS VP software and a Phenomenex Luna C18 (2) column (Torrance, CA, USA) (10 μm, 250 mm × 10 mm i.d.). The mobile phase used was 9:1 MeOH (Merck): H_2O with a flow rate of 6.0 ml/min followed by detection at 282 nm. The structure of 4-NC was deduced by nuclear magnetic resonance ^1H (300 MHz), ^{13}C (75 MHz) and spectral features were compared with published values (Kijjoa et al., 1980; Ropke et al., 2006).

Cell culture

The metastatic melanoma cell lines used in this work were kindly donated by Dr. María S. Soengas (Melanoma Group, CNIO, Spain). They are denominated as: SK-Mel-19, SK-Mel-28, SK-Mel-29, SK-Mel-103, SK-Mel-147, UACC-62, UACC- 257 and WM-1366. Primary cultures of skin cells (keratinocytes, melanocytes and fibroblasts) were obtained from the foreskins of University Hospital (Hospital Universitário – HU-USP) patients, donated by Dr. Linda Maximiano. To this end, the project has undergone review and approval by the Ethics Committee of HU (HU no. CEP Case 943/09). Melanoma cells and fibroblasts were grown in Dulbecco's modified Eagle's medium (DMEM) supplemented with 10% fetal bovine serum (FBS), 50 U/ml penicillin and 50 μg/ml streptomycin. The keratinocytes were maintained in Epilife media (SKU # M-EPICF-500; Cascade Biologics, Portland, OR, USA) supplemented with human keratinocyte growth supplement (HKGS – SKU # S-001; Cascade Biologics). The melanocytes were maintained in 254CF media (SKU # M-500-254CF; Cascade Biologics) supplemented with human melanocyte growth supplement (HMGS – SKU # S-002-5; Cascade Biologics). All cells were maintained at 37°C under 5% CO_2 atmosphere. The pure 4-NC was dissolved in 100% ethanol at a concentration of 10 mM and stored at –20°C. The ethanol concentration never exceeded 0.1% in culture and showed 100% cell viability when used as a control.

Measurement of cell viability

A total of 5×10^4 cells from each cell line were plated for a 24-h attachment period followed by treatment with 4-NC (10 or 30 μM). Cell viability was assessed by standard Trypan Blue exclusion assay 24 h after incubation with the compound by counting live versus dead cells on a hemocytometer chamber using Trypan Blue (0.4% in phosphate-buffered saline, PBS) exclusion staining. The assay was done in quadruplicate. IC_{50} values (i.e. the concentration that inhibited cell growth by 50% compared with untreated controls) were obtained by non-linear regression analysis with GRAPHPAD PRISM (GraphPad Software, San Diego, CA, USA).

Analysis of the activity of enzymes involved in cellular antioxidant system

The melanoma cell line SK-Mel-103 and fibroblasts were plated at 8×10^5 cells in a 100 mm^2 plate. After a 24-h attachment period, 4-NC was added for a 24-h incubation period. The total protein was extracted in phosphate buffer containing 0.5 mM EDTA. For measurement of catalase activity, 100 mM EDTA plus Tris buffer pH 8.0 were added to 30 μg of sample. Following the addition of 6% (v/v) H_2O_2 solution, samples were read for 5 min (at 1-min intervals) at 230 nm (30°C). The activity value represents the amount of catalase required to hydrolyze 1 μmol H_2O_2/min. For SOD activity measurement, 0.05 M phosphate buffer (pH 7.8) solution containing 1 mg/ml xanthine, 1 mg/ml KCN, 100 mM EDTA and 2 mg/ml cytochrome *c* were added to the samples described above. To finish, xanthine oxidase (1.82 U/ml) was added and the samples read for 5 min (at 1-min intervals) at 550 nm (25°C). The activity value represents the amount of SOD required to inhibit 50% of the xanthine oxidase reaction. All readings were made in a BIOTEK plate reader (Bio Tek Instruments Inc., Winooski, VT, USA).

DNA extraction and hydrolysis

Cell DNA was isolated as described in the Puregene Gentra® protocol (Qiagen, Valencia, CA, USA) with some modifications. Briefly, cells of one culture dish (approximately 1×10^7 cells) were resuspended in the culture medium without FBS and centrifuged at 300 *g* for 5 min. The supernatant was discarded and the pellet was resuspended in 3 ml of Puregene cell lysis solution. RNase A (30 μl of a 15 mg/ml solution) was added to the cell lysate and, after 1 h at 37°C, protein was precipitated by addition of 1 ml of Puregene protein precipitation solution and centrifugation at 2000 *g* for 10 min. The supernatant was poured into a tube containing 5 ml of cold 2-propanol and the precipitated DNA was collected by centrifugation at 2000 *g* for 3 min. The DNA was then washed with 3 ml of 70% ethanol, dried, and resuspended in 200 μl of 0.1 mM desferoxamine solution. DNA concentration was determined by measuring UV absorption at 260 nm, and DNA purity was assessed by the UV absorbance ratio at 260/280 nm. For the enzymatic hydrolysis, 30-μg aliquots of DNA samples in 0.1 mM desferoxamine solution were added to 3.75 μl of Tris–HCl/$MgCl_2$ buffer (200 mM, pH 7.4), 6.5 units of DNase I, and 2000 fmol of [$^{15}N_5$]8-oxodGuo. The samples were incubated at 37°C for 1 h. Phosphodiesterase I (0.005 units) and alkaline phosphatase (6.5 units) were then added and the incubation was continued for another 1 h at 37°C. At the end of the second incubation, the final volume (100 μl) was centrifuged at 9300 *g* for 10 min. Aliquots of 50 μl were injected in the HPLC-ESI-MS/MS-MRM system for quantitation of 8-oxodGuo. Concomitantly, 6 μl of the hydrolyzed DNA solution was injected in the HPLC-UV system for quantitation of 5-methyl-dCyd and normal deoxynucleosides. The analytical systems and the chromatographic conditions are described below.

8-Oxo-7,8-dihydro-2′-deoxyguanosine analysis through HPLC-ESI-MS/MS

The levels of 8-oxodGuo in DNA samples were analyzed by HPLC-ESI-MS/MS-MRM. The analytical system consisted of an Agilent 1200 series HPLC (Wilmington, DE, USA) equipped with a binary pump (Agilent 1200 G1312B), an isocratic pump (Agilent 1200 G1310A), a column oven (Agilent 1200 G1316B), a diode array detector (Agilent 1200 DAD G1315C) and an auto sampler (G1367C Agilent 1200) interfaced with a Linear Quadrupole Ion Trap mass spectrometer, Model 4000 QTRAP (Applied Biosystems/MDS Sciex Instruments, Foster City, CA, USA). The ESI-MS parameters were set in the positive ion mode as follows: curtain gas, 20 psi; ion source gas, 50 psi; collision-induced dissociation gas, low; ESI probe temperature, 550°C; declustering potential, 46 V; entrance potential, 10 V; collision energy, 17 eV; collision cell exit potential, 52 V; and ion spray voltage, 5500 V. Analyses were carried out with multiple reaction monitoring (MRM) using the *m/z* 284 (MH^+) → *m/z* 168 (MH^+-2′-deoxyribose+H) fragmentation for 8-oxodGuo and *m/z* 289 (MH^+) → *m/z* 173 (MH^+-2′-deoxyribose+H) fragmentation for [$^{15}N_5$]8-oxodGuo. The calibration curve was constructed at the interval of 0–250 fmol of 8-oxodGuo, with a fixed amount of [$^{15}N_5$]8-oxodGuo (1000 fmol). The data were acquired and processed using ANALYST software 1.4 (Applied Biosystems/MDS Sciex). The molar fraction 8-oxodGuo/dGuo present in each DNA sample was determined. The following chromatography conditions were used for the analyses. A 50 × 2.0 mm i.d., 2.5 μm, Luna C18(2)-HST column (Phenomenex) with a C18(2) security guard cartridge 4.0 × 3.0 mm i.d. (Phenomenex) was eluted with a gradient of 0.1% formic acid (solvent A) and methanol containing 0.1% formic acid (solvent B) at a flow rate of 150 μl/min and at 25°C, as follows: from 0 to 25 min, 0–15% of solvent B; 25–28 min, 15–80% of solvent B; 28–31 min, 80% of solvent B; 31–33 min, 80–0% of solvent B; 33–46 min, 0% of solvent B. The first 16 min of eluant was directed to waste and the 16–32 min fraction was diverted to a second column [150 × 2.0 mm i.d., 3.0 μm, Luna C18(2)] connected to the ESI source and conditioned by a third isocratic pump with a solution of 15% methanol in water containing 0.1% formic acid. The lesion 8-oxodGuo eluted from the second column at approximately 36 min. All solvents used were previously filtered and degassed.

Analysis of DNA global methylation through HPLC-UV

The quantitation of 5-methyl-dCyd and normal 2′-desoxynucleosides was carried out with a Shimadzu HPLC system equipped with two LC-20AT pumps, a photo diode array detector (PDA-20AV), an autoinjector (Proeminence SIL-20AC), and a column oven (CTO-10AS/VP) controlled by a CBM-20A communication module and the software LC-Solution. Elution system was as follows: a 250 mm × 4.6 mm i.d., 5 μm, Luna C18(2) column (Phenomenex) attached to a C18(2) guard column (4.0 × 3.0 mm i.d., 4 μm, Phenomenex), eluted with a gradient of formic acid 0.1% and CH_3OH (from 0 to 25 min, 0–18% CH_3OH; from 25 to 27 min, 18–0% CH_3OH; from 27 to 37 min, 0% CH_3OH) at a flow rate of 1 ml/min and 30°C. The PDA detector was set at 286 nm for 5-methyl-dCyd and at 260 nm for normal 2′-desoxynucleoside quantitation. Calibration curves were constructed at intervals of 0.005–0.05 nmol for 5-methyl-dCyd and 0.05–1 nmol for dCyd and dGuo. The percentage of DNA global methylation was calculated using the following equation: 5-methyl-dCyd (%) = nmol 5-methyl-dCyd × 100/(nmol 5-methyl-dCyd + nmol dCyd).

ROS detection by lucigenin

To assess ROS production, we used a chemiluminescent lucigenin probe for superoxide anion detection. Specifically, 10^6 cells were plated and then collected by trypsinization after 24 h of 4-NC treatment. The cells were centrifuged (1610 *g* for 5 min. TA), washed with PBS containing 0.5% glucose, re-centrifuged (1610 *g* for 5 min. TA) and diluted with PBS-0.5% glucose in the presence or absence of 4-NC, followed by addition of 0.1 mM lucigenin (bis-*N*-methylacridiniumnitrate). Subsequently, the cells were placed in a 96-well white opaque plate and the luminescence was read in a Berthold 9505 luminometer (EG & Instruments GmbH, Munich, Germany) every 2 min. Results were integrated and subsequently analyzed in Microsoft EXCEL.

2′,7′-Dichlorofluorescein-diacetate

Alternatively, for ROS detection, 2×10^5 cells were seeded and samples were collected by trypsinization after 30 min, 2, 4, 6 and 12 h of incubation with 4-NC and 100 μM DCFH-DA (2′,7′-dichlorfluorescein-diacetate; Sigma, St. Louis, MO, USA). The pellets were washed and resuspended in PBS for analysis by flow cytometry. The fluorescence of DCFH-DA was measured in the FITC-FL1 channel (530/30 nm green fluorescence) of a BD FACs CANTO TM II (BD, Biosciences, Bedford, MA) flow cytometer and results were integrated and subsequently analyzed in Microsoft EXCEL.

Flow cytometric analysis of γ-H2AX

Cells treated with 4-NC (30 μM) were collected by trypsinization and fixed in fresh 2% formaldehyde at 4°C for 15 min. The fixed cells were centrifuged at 11450 *g* for 10 min and washed once with PBS. They were resuspended in ice-cold 70% ethanol and kept at −20°C overnight. The cells were centrifuged and permeated/blocked in PBS containing 0.2% Triton X-100 and 1% bovine serum albumin (BSA-T-PBS) at room temperature for 5 min. Cells were incubated with anti-phospho Ser139-H2AX mouse monoclonal antibody (05-636, 1/300, Millipore, Billerica, MA, USA) at room temperature for 1 h. After washing in BSA-T-PBS, they were incubated with anti-mouse Alexa Fluor® 488-conjugated IgG goat anti-

body (A-10684, 1/200, Invitrogen, Carlsbad, CA, USA) at room temperature for 1 h. The fluorescence intensity of FITC was determined using a FACs CANTO TM II flow cytometer (BD Biosciences, Bedford, MA, USA) and the results were analyzed with FLOWJO software v. 8.8.2 (Tree Star, Ashland, OR, USA). At least 10 000 cells per sample were analyzed.

Western blotting

To detect alterations in protein levels, 2×10^6 cells were treated with 4-NC (10 or 30 μM), Doxorubicin (0.6 μg/ml; Fisher, Fair Lawn, NJ, USA), bortezomib (50 nM, Millennium Pharmaceuticals Inc., Osaka, Japan), MG132 (5 μM; C2211, Sigma-Aldrich Corp., St. Louis, MO, USA) or z-VAD-fmk (20 nM; Millennium Pharmaceuticals Inc.) and harvested 24 h after treatment. Total cell lysates were obtained with Laemmli Buffer (10% SDS, 0.0625 M Tris-HCl pH 6.8, 10% glycerol, and 5% 2-beta-mercaptoethanol) extraction. Total protein, 30 μg was subjected to electrophoresis in 12, 15 or 4–15% gradient SDS gels under reducing conditions, and subsequently transferred to polyvinylidene difluoride (PVDF) membranes (Hybond-P, Amersham Pharmacia Biotech, Piscataway, NJ, USA). The membranes were incubated with the following antibodies: actin (A5316, Sigma); Bax (2772, Cell Signaling, Beverly, MA, USA); Bcl-2 (2876. Cell Signaling), Bcl-xL (610211, BD Biosciences); Bid (2002, Cell Signaling), caspase-3 (9662, Cell Signaling), caspase-9 (9502, Cell Signaling), Mcl-1 (SC-819, Santa Cruz, St. Louis, MO, USA); Noxa (114C307, Calbiochem/Merck KGaA, Darmstadt, Germany); p53 (VP-P955, Vector, Burlingame, CA, USA), tubulin (T6199; Sigma), and ubiquitin (SPA205, Stress Gene, San Diego, CA, USA). Protein bands were detected by enhanced chemiluminescence system ECL (Amersham Pharmacia Biotech).

Determination of mitochondrial membrane potential by flow cytometry

To determine the mitochondrial membrane potential, 2×10^5 cells were plated and, after a 24-h attachment period, 4-NC was added as described above, followed by addition of DiCO 6(3) (3,3′-dihexyloxacarbocyanine iodide, Sigma) 30 min prior to collection. Samples were collected by trypsinization. The pellets were washed and resuspended in PBS for flow-cytometric analysis. The fluorescence of DiCO 6(3) was measured in the FITC-FL1 channel (green fluorescence, excitation at 488 nm and emission at 525 nm) of a BD FACs CANTO TM II (BD Biosciences) flow cytometer. Results were integrated and subsequently analyzed in Microsoft EXCEL.

Proteasome inhibition assay

The proteasome activity was measured by the 20S Proteasome Activity Assay Kit (APT 280; Chemicon-Millipore, Billerica, MA, USA), following the manufacturer's instructions. The assay is based on detection of the fluorophore 7-amino-4-methylcoumarin (AMC) after cleavage from the labeled substrate LLVY-AMC. After treatment with 4-NC for 24 h, the cells were collected by scraping and were washed twice with cold PBS. The pellet was lysed with 0.5 ml lysis buffer [50 mM HEPES (pH 7.5), 5 mM EDTA, 150 mM NaCl and 1% Triton X-100] for 30 min on ice, with vortexing at 10-min intervals. The lysate was centrifuged at 23900 *g* for 15 min at 4°C. As samples, 30 μg of the lysates were used and the proteasome substrate was added. Lactacystin (250 nM) was added to the control lysate as a negative control 15 min prior to the proteasome substrate addition. Samples were incubated for 1 h at 37°C and the free AMC fluorescence was quantified at 380/460 nm in a Bio Tek® fluorometer (Bio Tek Instruments Inc.). As an internal control of the experiment, the drug lactacystin was used in the NT cell extracts to show that the cells have functional proteasome activity (data not shown).

Lentiviral infections

To inhibit Noxa expression, the melanoma cell line SK-Mel-103 was infected with shRNA lentiviral particles designed to downregulate Noxa, which were kindly donated by Dr. María S. Soengas (CNIO, Spain). The sequences of the shRNA lentiviral vectors used in this work have been reported previously (Fernández et al., 2005). Treatment with 4-NC was initiated 3 days after infection with virus containing shRNA sequences.

Artificial skin reconstruction

To manufacture the artificial skin reconstructs, we followed Boccardo et al. (2004) with the modifications described below. The dermal equivalent was prepared with 1.5×10^5 fibroblasts embedded in a type I collagen (BD Biosciences) matrix. After dermal equivalent polymerization, 1.5×10^5 keratinocytes, 10^4 melanocytes and 10^4 melanoma cells were plated above the dermal layer. Following contraction of the collagen gel, the entire structure was transferred to a steel grid to allow for an air–liquid interface while maintaining contact with the raft medium consisting of 67.5% DME, 22.5% Ham's F12; 10% fetal calf serum, 5 μg/ml apo-transferrin (T-1147; Sigma), 5 μg/ml insulin (I-1882; Sigma), 0.4 mg/ml hydrocortisone 21-hemisuccinate (H-4881; Sigma), 1 ng/ml EGF (human epidermal growth factor, 13247-010; Gibco/Invitrogen) and 0.1 nM cholera toxin (3012; Sigma). After 2 weeks at the interface, 4-NC was added for an additional 72 h. The skin reconstructs were washed with PBS pH 7.4 and embedded in paraffin for histological analysis.

Immunohistochemical staining

After deparaffinization and rehydration, antigen retrieval was carried out with Tris-EDTA, pH 9.0 (S3307; DAKO, Carpinteria, CA, USA), in a water bath heated with steam and held at 97°C for 30 min. Slides were cooled to room temperature for 20 min, washed with distilled water and TBST buffer (Tris-buffered saline with 0.01% Tween-20, 3306, Dako®). The slides were blocked with 2% BSA for 2 h at 37°C. The primary antibodies keratin 14 (ab7800 Abcam, Cambridge, MA, USA) and involucrin (ab27495; Abcam) were diluted 1:100 in 2% BSA. The Fast-Red Substrate Kit (ab64253; Abcam) or ARK (Animal Research Kit, K3954– Dako) were used for detection purposes. Primary antibody was omitted for negative controls.

Statistical analysis

All data is expressed as the mean ± SEM, except 8-oxodGuo, which are expressed as the mean ± SD. GRAPH PAD INSTAT software (version 3.01 for Windows XP; Graph Pad Software, San Diego, CA, USA) was used to perform statistical analyses. One-way ANOVA with a Tukey–Kramer multiple comparison test was used for data analyses. We used the correlation analyses potentially to identify causal associations between variables. For cytotoxicity experiments, the statistical analyses were performed using GRAPH PAD PRISM 4 (version 4.00 for Windows Vista; Graph Pad Software) software, and the two-way ANOVA test was performed for data analyses.

Acknowledgements

We are especially grateful to Dr. Gilles Landman (Pathology Department, Universidade Federal de São Paulo, Brazil) for evaluation of artificial skin reconstructs, and Dr. Linda Maximiano for the foreskin donation (Hospital universitário, Universidade de São Paulo, Brazil). We also thank Dr. Monique Verhaegen (Dermatology Department, University of Michigan, USA), for the critical reading of the manuscript and her precious suggestions. We thank Prof. Paolo Di Mascio (Instituto de Química, Universidade de São Paulo, Brazil) for the HPLC-ESI-MS/MS equipment. We are also grateful to Dr. Car-

los F. Menck (Bioscience Institute, Universidade de São Paulo, Brazil) and Dr. Francisco Laurindo (INCOR, Universidade de São Paulo, Brazil) for the donation of some reagents used in the present work. This study was supported by FAPESP (2006/50479-7, 2006/60930-8, 2008/58817-4, 2009/54816-6 2010/50157-5), CNPq, INCT-if CNPq, CAPES and PRP-USP.

References

Amiri, K.I., Horton, L.W., LaFleur, B.J., Sosman, J.A., and Richmond, A. (2004). Augmenting chemosensitivity of malignant melanoma tumors via proteasome inhibition: implication for bortezomib (VELCADE, PS-341) as a therapeutic agent for malignant melanoma. Cancer Res. *64*, 4912–4918.

Averill-Bates, D.A., Ke, Q., Tanel, A., Roy, J., Fortier, G., and Agostinelli, E. (2008). Mechanism of cell death induced by spermine and amine oxidase in mouse melanoma cells. Int. J. Oncol. *32*, 79–88.

Barros, S.B.M., Teixeira, D.S., Aznar, A.E., Moreira Jr, J.A., Ishii, I., and Freitas, P.C.D. (1996). Antioxidant activity of ethanolic extracts of *Pothomorphe umbellata* L. Miq. Ciência Culturu. *48*, 114–116.

Bianchini, F., Jaeckel, A., Vineis, P., Martinez-Garcia, C., Elmstahl, S., Van Kappel, A.L., Boeing, H., Ohshima, H., Riboli, E., and Kaaks, R. (2001). Inverse correlation between alcohol consumption and lymphocyte levels of 8-hydroxydeoxyguanosine in humans. Carcinogenesis *22*, 885–890.

Boccardo, E., Noya, F., Broker, T.R., Chow, L.T., and Villa, L.L. (2004). HPV-18 confers resistance to TNF-alpha in organotypic cultures of human keratinocytes. Virology *328*, 233–243.

Brohem, C.A., Sawada, T.C., Massaro, R.R. et al. (2009). Apoptosis induction by 4-nerolidylcatechol in melanoma cell lines. Toxicol. In Vitro *23*, 111–119.

Brohem, C.A., Cardeal, L.B., Tiago, M., Soengas, M.S., Barros, S.B., and Maria-Engler, S.S. (2010). Artificial skin in perspective: concepts and applications. Pigment Cell Melanoma Res. *24*, 35–50.

Cadet, J., Douki, T., and Ravanat, J.L. (2008). Oxidatively generated damage to the guanine moiety of DNA: mechanistic aspects and formation in cells. Acc. Chem. Res. *41*, 1075–1083.

Celeste, A., Fernandez-Capetillo, O., Kruhlak, M.J., Pilch, D.R., Staudt, D.W., Lee, A., Bonner, R.F., Bonner, W.M., and Nussenzweig, A. (2003). Histone H2AX phosphorylation is dispensable for the initial recognition of DNA breaks. Nat. Cell Biol. *5*, 675–679.

Chandan, R. (2002). Trade in health services. Bull. World Health Org. *80*, 158–163.

Chao, M.R., Yen, C.C., and HU, C.W. (2008). Prevention of artifactual oxidation in determination of cellular 8-oxo-7,8-dihydro-2′-deoxyguanosine by isotope-dilution LC-MS/MS with automated solid-phase extraction. Free Radical Biol. Med. *44*, 464–473.

Chen, G., Wang, Y., Garate, M., Zhou, J., and Li, G. (2009). The tumor suppressor ING3 is degraded by SCF(Skp2)-mediated ubiquitin-proteasome system. Oncogene *29*, 1498–1508.

Chioni, A.M., and Grose, R. (2008). Organotypic modelling as a means of investigating epithelial-stromal interactions during tumourigenesis. Fibrogenesis Tissue Repair *1*, 8.

Chuang, C.Y., Liu, H.C., Wu, L.C., Chen, C.Y., Chang, J.T., and Hsu, S.L. (2010). Gallic acid induces apoptosis of lung fibroblasts via a reactive oxygen species-dependent ataxia telangiectasia mutated-p53 activation pathway. J. Agric. Food Chem. *58*, 2943–2951.

Crusio, K.M., King, B., Reavie, L.B., and Aifantis, I. (2010). The ubiquitous nature of cancer: the role of the SCF(Fbw7) complex in development and transformation. Oncogene *29*, 4865–4873.

Demidem, A., Morvan, D., Papon, J., De Latour, M., and Madelmont, J.C. (2010). Cystemustine induces redifferentiation of primary tumors and confers protection against secondary tumor growth in a melanoma murine model. Cancer Res. *61*, 2294–2300.

Desmarchelier, C., Slowing, K., and Ciccia, G. (2000). Anti-inflammatory activity of *Pothomorphe peltata* leaf methanol extract. Fitoterapia *71*, 556–558.

Dong, L.F., Swettenham, E., Eliasson, J. et al. (2007). Vitamin E analogues inhibit angiogenesis by selective induction of apoptosis in proliferating endothelial cells: the role of oxidative stress. Cancer Res. *67*, 11906–11913.

ESCODD (European Standards Committee on Oxidative DNA Damage). (2002). Comparative analysis of baseline 8-oxo-7,8-dihydroguanine in mammalian cell DNA, by different methods in different laboratories: an approach to consensus. Carcinogenesis *23*, 1129–1133.

ESCODD (European Standards Committee on Oxidative DNA Damage), Gedik, C.M., and Collins, A. (2004). Establishing the background level of base oxidation in human lymphocyte DNA: results of an interlaboratory validation study. FASEB J. *18*, 82–105.

Fernández, Y., Verhaegen, M., Miller, T.P., Rush, J.L., Steiner, P., Opipari Jr, A.W., Lowe, S.W., and Soengas, M.S. (2005). Differential regulation of noxa in normal melanocytes and melanoma cells by proteasome inhibition: therapeutic implications. Cancer Res. *65*, 6294–6304.

Fernández, Y., Miller, T.P., Denoyelle, C., Esteban, J.A., Tang, W.H., Bengston, A.L., and Soengas, M.S. (2006). Chemical blockage of the proteasome inhibitory function of bortezomibe: impact on tumor cell death. J. Biol. Chem. *281*, 1107–1118.

Flaherty, K.T., Puzanov, I., Kim, K.B. et al. (2010). Inhibition of mutated, activated BRAF in metastatic melanoma. N. Engl. J. Med. *363*, 809–819.

Gaddameedhi, S., and Sancar, A. (2011). Melanoma and DNA damage from a distance (farstander effect). Pigment Cell Melanoma Res. *24*, 3–4.

Girnita, L., Girnita, A., Brodin, B. et al. (2000). Increased expression of insulin-like growth factor I receptor in malignant cells expressing aberrant p53: functional impact. Cancer Res. *60*, 5278–5283.

Gray-Schopfer, V., Wellbrock, C., and Marais, R. (2007). Melanoma biology and new targeted therapy. Nature *445*, 851–857.

Greinert, R. (2009). Skin cancer: new markers for better prevention. Pathobiology *76*, 64–81.

Gustafson, K.R., Cardellina, J.H., McMahon, J.B., Pannell, L.K., Cragg, G.M., and Boyd, M.R. (1992). HIV inhibitory natural products. The peltatols, novel HIV-inhibitory catechol derivatives from *Pothomorphe peltata*. J. Org. Chem. *57*, 2809–2811.

Haapajarvi, T., Pitkanen, K., and Laiho, M. (1999). Human melanoma cell line UV responses show independency of p53 function. Cell Growth Differ. *10*, 163–171.

Hersey, P., and Zhang, X.D. (2001). How melanoma cells evade trail-induced apoptosis. Nat. Rev. Cancer *1*, 142–150.

Hodi, F.S., O'Day, S.J., McDermott, D.F. et al. (2010). Improved survival with ipilimumab in patients with metastatic melanoma. N. Engl. J. Med. *363*, 711–723.

Ibrahim, N., and Haluska, F.G. (2009). Molecular pathogenesis of cutaneous melanocytic neoplasms. Annu. Rev. Pathol. *4*, 551–579.

James, S.J., Pogribny, I.P., Pogribna, M., Miller, B.J., Jernigan, S., and Melnyk, S. (2003). Mechanisms of DNA damage, DNA hypomethylation, and tumor progression in the folate/methyl-deficient rat model of hepatocarcinogenesis. J. Nutr. *133*, 3740S–3747S.

Jesenberger, V., and Jentsch, S. (2002). Deadly encounter: ubiquitin meets apoptosis. Nat. Rev. Mol. Cell Biol. *3*, 112–121.

Kijjoa, A., Giesbrecht, A.M., Akisue, M.K., Gottlieb, O.R., and Gottlieb, H.E. (1980). 4-Nerolidylcathecol from *Pothomorphe umbellata*. Planta Med. *39*, 85–87.

Koch, O.R., Pani, G., Borrello, S., Colavitti, R., Cravero, A., Farrè, S., and Galeotti, T. (2004). Oxidative stress and antioxidant defenses in ethanol-induced cell injury. Mol. Aspects Med. *25*, 191–198.

Lecis, D., Drago, C., Manzoni, L. et al. (2010). Novel SMAC-mimetics synergistically stimulate melanoma cell death in combination with TRAIL and bortezomib. Br. J. Cancer *102*, 1707–1716.

Li, H.L., Chen, D.D., Li, X.H., Zhang, H.W., Lu, Y.Q., Ye, C.L., and Ren, X.D. (2002). Changes of NF-kB, p53, Bcl-2 and caspase in apoptosis induced by JTE-522 in human gastric adenocarcinoma cell line AGS cells: role of reactive oxygen species. World J. Gastroenterol. *8*, 431–435.

Li, G.X., Chen, Y.K., Hou, Z. et al. (2010). Pro-oxidative activities and dose-response relationship of (–)-epigallocatechin-3-gallate in the inhibition of lung cancer cell growth: a comparative study in vivo and in vitro. Carcinogenesis *31*, 902–910.

Mangal, D., Vudathala, D., Park, J.H., Lee, S.H., Penning, T.M., and Blair, I.A. (2009). Analysis of 7,8-dihydro-8-oxo-2′-deoxyguanosine in cellular DNA during oxidative stress. Chem. Res. Toxicol. *22*, 788–797.

Markovic, S.N., Geyer, S.M., Dawkins, F. et al. (2005). A phase II study of bortezomib in the treatment of metastatic malignant melanoma. Cancer *103*, 2584–2589.

Merle, P., Morvan, D., Caillaud, D., and Demidem, A. (2008). Chemotherapy-induced bystander effect in response to several chloroethylnitrosoureas: an origin independent of DNA damage? Anticancer Res. *28*, 21–27.

Meyskens Jr, F.L., McNulty, S.E., Buckmeier, J.A., Tohidian, N.B., Spillane, T.J., Kahlon, R.S., and Gonzalez, R.I. (2001). Aberrant redox regulation in human metastatic melanoma cells compared to normal melanocytes. Free Radic Biol Med. *31*, 799–808.

Miller, L.A., Goldstein, N.B., Johannes, W.U., Walton, C.H., Fujita, M., Norris, D.A., and Shellman, Y.G. (2009). H3 mimetic ABT-737 and a proteasome inhibitor synergistically kill melanomas through Noxa-dependent apoptosis. J Invest Dermatol. *129*, 964–971.

Mousavi-Shafaei, P., Ziaee, A.A., and Zangemeister-Wittke, U. (2009). Increased cytotoxicity of cisplatin in SK-MEL 28 melanoma cells upon down-regulation of melanoma inhibitor of apoptosis protein. Iran. Biomed. J. *13*, 27–34.

Nakazato, T., Ito, K., Ikeda, Y., and Kizaki, M. (2005). Green tea component, catechin, induces apoptosis of human malignant B cells via production of reactive oxygen species. Clin. Cancer Res. *11*, 6040–6049.

Nihal, M., Ahmad, N., Mukhtar, H., and Wood, G.S. (2005). Anti-proliferative and proapoptotic effects of (–)-epigallocatechin-3-gallate on human melanoma: possible implications for the chemoprevention of melanoma. Int. J. Cancer *114*, 513–521.

Nikiforov, M.A., Riblett, M., Tang, W.H. et al. (2007). Tumor cell-selective regulation of NOXA by c-MYC in response to proteasome inhibition. Proc. Natl Acad. Sci. U S A *104*, 19488–19493.

Nishikawa, M., Hyoudou, K., Kobayashi, Y., Umeyama, Y., Takakura, Y., and Hashida, M. (2005). Inhibition of metastatic tumor growth by targeted delivery of antioxidant enzymes. J. Control Rel. *109*, 101–107.

Oda, E., Ohki, R., Murasawa, H., Nemoto, J., Shibue, T., Yamashita, T., Tokino, T., Taniguchi, T., and Tanaka, N. (2000). Noxa, a BH3-only member of the Bcl-2 family and candidate mediator of p53-induced apoptosis. Science *288*, 1053–1058.

Pani, G., Koch, O.R., and Galeotti, T. (2009a). The p53-p66shc-manganese superoxide dismutase (MnSOD) network: a mitochondrial intrigue to generate reactive oxygen species. Int. J. Biochem. Cell Biol. *41*, 1002–1005.

Pani, G., Giannoni, E., Galeotti, T., and Chiarugi, P. (2009b). Redox-based escape mechanism from death: the cancer lesson. Antioxid. Redox Signal. *11*, 2791–2806.

Paraiso, K.H., Fedorenko, I.V., Cantini, L.P., Munko, A.C., Hall, M., Sondak, V.K., Messina, J.L., Flaherty, K.T., and Smalley, K.S. (2010). Recovery of phospho-ERK activity allows melanoma cells to escape from BRAF inhibitor therapy. Br. J. Cancer *102*, 1724–1730.

Pérez-Galán, P., Roué, G., Villamor, N., Montserrat, E., Campo, E., and Colomer, D. (2006). The proteasome inhibitor bortezomib induces apoptosis in mantle-cell lymphoma through generation of ROS and Noxa activation independent of p53 status. Blood *107*, 257–264.

Ploner, C., Kofler, R., and Villunger, A. (2008). Noxa: at the tip of the balance between life and death. Oncogene *27*, S84–S92.

Podhorecka, M., Skladanowski, A., and Bozko, P. (2010). H2AX phosphorylation: its role in DNA damage response and cancer therapy. J. Nucl. Acids *Pii*, 920161.

Ravanat, J.L., Douki, T., Duez, P., Gremaud, E., Herbert, K., Hofer, T., Lasserre, L., Saint-Pierre, C., Favier, A., and Cadet, J. (2002). Cellular background level of 8-oxo-7,8-dihydro-2′-deoxyguanosine: an isotope based method to evaluate artefactual oxidation of DNA during its extraction and subsequent work-up. Carcinogenesis *23*, 1911–1918.

Ribeiro, D.A., Salvadori, D.M., and Marquez, M.E. (2005). Abnormal expression of bcl-2 and bax in rat tongue mucosa during the development of squamous cell carcinoma induced by 4-nitroquinoline 1-oxide. Int. J. Exp. Pathol. *86*, 375–381.

Rieber, M., and Rieber, M.S. (1999). Tumor suppression without differentiation or apoptosis by antisense cyclin D1 gene transfer in K1735 melanoma involves induction of p53, p21WAF1 and superoxide dismutases. Cell Death Differ. *6*, 1209–1215.

Roberti, A., Rizzolio, F., Lucchetti, C., de Leval, L., and Giordano, A. (2011). Ubiquitin-mediated protein degradation and methylation-induced gene silencing cooperate in the inactivation of the INK4/ARF locus in Burkitt lymphoma cell lines. Cell Cycle *10*, 127–134.

Roberts, R.J. (1995). On base flipping. Cell *82*, 9–12.

Ropke, C.D., Kaneko, T.M., Rodrigues, R.M., da Silva, V.V., Barros, S., Sawada, T.C., Kato, M.J., and Barros, S.B. (2002). Evaluation of percutaneous absorption of 4-nerolidylcathecol from four topical formulations. Int. J. Pharm. *249*, 109–116.

Ropke, C.D., da Silva, V.V., Kera, C.Z., Miranda, D.V., de Almeida, R.L., Sawada, T.C., and Barros, S.B. (2006). *In vitro* and *in vivo* inhibition of skin matrix metalloproteinases by *Pothomorphe umbellata* root extract. Photochem. Photobiol. *82*, 439–442.

Seeger, J.M., Schmidt, P., Brinkmann, K. et al. (2010). The proteasome inhibitor bortezomib sensitizes melanoma cells toward adoptive CTL attack. Cancer Res. *70*, 1825–1834.

Sies, H. (1993). Strategies of antioxidant defense. Eur. J. Biochem. *215*, 213–219.

Silva, R.A.D. (1926). Pharmacopéia dos Estados Unidos do Brasil. (São Paulo: Nacional), 649.

Smalley, K.S., and Sondak, V.K. (2010). Melanoma – an unlikely poster child for personalized cancer therapy. N. Engl. J. Med. *363*, 876–878.

Soengas, M.S., and Lowe, S.W. (2003). Apoptosis and melanoma chemoresistance. Oncogene *22*, 3138–3151.

Sorolla, A., Yeramian, A., Dolcet, X. et al. (2008). Effect of proteasome inhibitors on proliferation and apoptosis of human cutaneous melanoma-derived cell lines. Br. J. Dermatol. *158*, 496–504.

Su, Y., Amiri, K.I., Horton, L.W., Yu, Y., Ayers, G.D., Koehler, E., Kelley, M.C., Puzanov, I., Richmond, A., and Sosman, J.A. (2010). A phase I trial of bortezomib with temozolomide in

patients with advanced melanoma: toxicities, antitumor effects, and modulation of therapeutic targets. Clin. Cancer Res. *16*, 348–357.

Tawbi, H., and Nimmagadda, N. (2009). Targeted therapy in melanoma. Biologics *3*, 475–484.

Thomas, N.E., Edmiston, S.N., Alexander, A. et al. (2007). Number of nevi and early-life ambient UV exposure are associated with BRAF-mutant melanoma. Cancer Epidemiol Biomarkers Prev. *16*, 991–997.

Tormo, D., Checińska, A., Alonso-Curbelo, D. et al. (2009). Targeted activation of innate immunity for therapeutic induction of autophagy and apoptosis in melanoma cells. Cancer Cell *16*, 103–114.

Verhaegen, M., Bauer, J.A., Martín de la Vega, C. et al. (2006). A novel BH3 mimetic reveals a mitogen-activated protein kinase-dependent mechanism of melanoma cell death controlled by p53 and reactive oxygen species. Cancer Res. *66*, 11348–11359.

Wolter, K.G., Verhaegen, M., Fernández, Y., Nikolovska-Coleska, Z., Riblett, M., de la Vega, C.M., Wang, S., and Soengas, M.S. (2007). Therapeutic window for melanoma treatment provided by selective effects of the proteasome on Bcl-2 proteins. Cell Death Differ. *14*, 1605–1616.

Yauk, C., Polyzos, A., Rowan-Carroll, A. et al. (2008). Germ-line mutations, DNA damage, and global hypermethylation in mice exposed to particulate air pollution in an urban/industrial location. PNAS *105*, 605–610.

Yoshino, M., Haneda, M., Naruse, M., Htay, H.H., Iwata, S., Tsubouchi, R., and Murakami, K. (2002). Prooxidant action of gallic acid compounds: copper-dependent strand breaks and the formation of 8-hydroxy-2 O-deoxyguanosine in DNA. Toxicol. *In Vitro 16*, 705–709.

Supporting information

Additional Supporting Information may be found in the online version of this article:

Figure S1. Fibroblasts are resistant to 4-NC action. Human dermal fibroblasts derived from foreskin (FF282, FF284, FF287 and HNF) were treated with 4-NC (10 and 30 μM) for 24 h.

Figure S2. Cell viability measured by Trypan Blue assay.

Figure S3. Evaluation of anti- and pro-apoptotic factors levels in melanocytes, keratinocytes and melanomas at lower concentrations of 4-NC.

Figure S4. Cell viability measured by MTT assay.

Figure S5. Effects of 4-NC on the dermal equivalent contraction (normal human fibroblasts (FHN) embedded in type I collagen gel).

Please note: Wiley-Blackwell are not responsible for the content or functionality of any supporting materials supplied by the authors. Any queries (other than missing material) should be directed to the corresponding author for the article.